A DISCRETE-TIME WAVELET TRANSFORM BASED ON A CONTINUOUS DILATION FRAMEWORK

Wei Zhao and Raghuveer M. Rao

Center for Imaging Science/
Electrical Engineering Department
Rochester Institute of Technology
79 Lomb Memorial Drive
Rochester, NY 14623-5603
Tel: (716)475-2185
Email: wxz1756@cis.rit.edu

ABSTRACT

In this paper we present a new form of wavelet transform. Unlike the continuous wavelet transform (CWT) or discrete wavelet transform (DWT), the mother wavelet is chosen to be a discrete-time signal and wavelet coefficients are computed by correlating a given discrete-time signal with continuous dilations of the mother wavelet. The results developed are based on the definition of a discrete-time scaling (dilation) operator through a mapping between the discrete and continuous frequencies. The forward and inverse wavelet transforms are formulated. The admissibility condition is derived, and examples of discrete-time wavelet construction are provided. The new form of wavelet transform is naturally suited for discrete-time signals and provides analysis and synthesis of such signals over a continuous range of scaling factors.

1. INTRODUCTION

The conventional discrete wavelet transform (DWT) [1, 2, 5, 6] provides a formulation over a dyadic set of scaling factors. However, in some wavelet applications, information at scaling factors other than those values on the dyadic grid is required. The conventional continuous wavelet transform (CWT) [2] provides information at scaling factors over a continuum. But, as the CWT is generally computed by using the samples of continuous-time wavelets, the computational complexity increases with the scaling factor. In both DWT and CWT, the set of wavelets are continuous-time signals. However, if the signal to be analyzed is inherently discrete-time, it is natural to choose a discrete-time signal as the mother wavelet and provide analysis and synthesis based on a set of wavelets which are discrete-time. In this paper we present a new formulation of wavelet transform in which the wavelets are all discrete-time signals, and continuous dilations of the mother wavelet are used to form a discrete-time wavelet transform over continuous scaling factors.

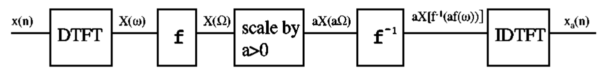

Figure 1: Block diagram of the discrete-time, continuous-dilation scaling operator. (I)DTFT: (inverse) discrete-time Fourier transform; f: frequency warping transform.

2. DISCRETE-TIME SCALING OPERATOR

Generally the scaling or dilation operation of a discrete signal $x(n)$ by an arbitrary factor is not well defined. It is difficult to obtain an interpretation of scaling in the discrete-time domain that is as unambiguous as that in the continuous-time domain. We present here a new approach for discrete-time scaling that can handle continuous scaling factors. We define the discrete-time scaling operator in a way that effectively amounts to converting $x(n)$ into a continuous-time signal through an invertible transform, applying the scaling operation to the continuous-time signal and finally mapping the signal back to the discrete-time domain. The definition is actually based on a warping transform in the frequency domain (Figure 1).

Definition 1 *A function $f(\;)$ is a discrete-time frequency (ω) to continuous-time frequency (Ω) warping transform if and only if:*

1. *In $\Omega = f(\omega)$, $\omega \in [-\pi, \pi]$ and Ω is the real line.*
2. *The transform is one-to-one.*

3. *$f(\,)$ is anti-symmetric about the origin, i.e. $f(-\omega) = -f(\omega)$. Furthermore, it is differentiable and monotonic in $[-\pi, \pi]$.*

4. *$f(0) = 0$.*

The defined discrete-time scaling operator gives the following input-output relationship in the frequency domain,

$$Y(\omega) = aX[\Lambda_a(\omega)], \tag{1}$$

where $X(\omega)$ and $Y(\omega)$ are discrete-time Fourier transforms of the input and output sequences, respectively, and

$$\Lambda_a(\omega) = f^{-1}[af(\omega)]. \tag{2}$$

3. DISCRETE-TIME CONTINUOUS-DILATION WAVELET TRANSFORMS

3.1. The Forward and Inverse Transforms

Let $\psi(n)$ be a discrete-time sequence and $\Psi(\omega)$ be its discrete-time Fourier transform defined by

$$\Psi(\omega) = \mathcal{G}[\psi(n)] = \sum_n \psi(n)e^{-j\omega n}, \tag{3}$$

where $\mathcal{G}$ denotes the discrete-time Fourier transform. Let

$$\Psi_a(\omega) = \sqrt{\Lambda_a'(\omega)}\Psi[\Lambda_a(\omega)], \tag{4}$$

where $'$ denotes the first derivative with respect to ω. Let

$$\psi_a(n) = \mathcal{G}^{-1}[\Psi_a(\omega)], \tag{5}$$

where $\mathcal{G}^{-1}$ is the inverse discrete-time Fourier transform. The discrete-time continuous-dilation wavelet transform (DCWT) is defined by choosing $\psi(n)$ as the mother wavelet and $\psi_a(n)$ as the wavelet at scale level a. It can be shown that $\psi(n)$ and $\psi_a(n)$ have the same energy. For a discrete-time sequence $x(n)$ and mother wavelet $\psi(n)$, the wavelet transform coefficients, $W_\psi(a,n)$, are computed as the inner products of $x(n)$ and translations of $\psi_a(n)$.

$$W_\psi(a,n) = \langle x(m), \psi_a(m-n)\rangle, \tag{6}$$

where $\langle\,\rangle$ denotes the inner product. The frequency domain representation of the forward DCWT is given by

$$W_\psi(a,n) = \frac{1}{2\pi}\int_{-\pi}^{\pi} X(\omega)\sqrt{\Lambda_a'(\omega)}\Psi^*[\Lambda_a(\omega)]e^{j\omega n}d\omega, \tag{7}$$

where $X(\omega)$ and $\Psi(\omega)$ are the discrete-time Fourier transforms of $x(n)$ and $\psi(n)$, and $*$ denotes the complex conjugate. The inverse discrete-time continuous-dilation wavelet transform (IDCWT) is given by

$$\hat{x}(n) = \frac{1}{C_\psi}\int_0^\infty \langle W_\psi(a,m), \hat{\psi}_a^*(m-n)\rangle da, \tag{8}$$

where

$$C_\psi = \int_{-\pi}^{\pi} f(\alpha)|\Psi(\alpha)|^2 d\alpha, \tag{9}$$

and

$$\hat{\psi}_a(n) = \mathcal{G}^{-1}\left[\frac{[f(\omega)]^2\sqrt{\Lambda_a'(\omega)}\Psi^*[\Lambda_a(\omega)]}{f'(\omega)}\right] \tag{10}$$

is the IDCWT wavelet at scale a. Note that different mother wavelets are used for the forward and inverse transforms. The relationship between the frequency spectrum, $\Psi(\omega)$, of the DCWT mother wavelet $\psi(n)$, and the frequency spectrum, $\hat{\Psi}(\omega)$, of the IDCWT mother wavelet $\hat{\psi}(n)$, is

$$\hat{\Psi}(\omega) = \frac{[f(\omega)]^2}{f'(\omega)}\Psi(\omega). \tag{11}$$

The admissibility condition [1] of the DCWT is

$$C_\psi = \int_{-\pi}^{\pi} f(\alpha)|\Psi(\alpha)|^2 d\alpha < \infty. \tag{12}$$

It is generally required that the frequency spectrum $\Psi(\omega)$ of the mother wavelet satisfies $\Psi(\pm\pi) = 0$. However, there is no restriction on the value of $\Psi(0)$.

3.2. Bilinear Transform Based DCWT and IDCWT

We discuss the DCWT and IDCWT for the case of bilinear transform [4] in which

$$f(\omega) = 2\tan(\omega/2). \tag{13}$$

For simplicity, we will only discuss constructions of real-valued, bandlimited wavelets and their corresponding DCWT and IDCWT. Let $\psi(n)$ be a discrete-time signal and $\Psi(\omega)$ be its discrete-time Fourier transform which satisfies

1. $|\Psi(\omega)| < \infty$ for all $\omega \in [-\pi, \pi]$.
2. $\Psi(\omega)$ is symmetric about the origin.
3. Bandlimitedness. $\Psi(\omega) = 0$ for $\omega \in [0, \omega_1]$ and $\omega \in [\omega_2, \pi]$, where $0 \le \omega_1 < \omega_2 \le \pi$.

It is easy to verify that $\psi(n)$ satisfies the admissibility condition and thus is a valid DCWT mother wavelet. The DCWT wavelet at scale a, $\psi_a(n)$, will then have a frequency spectrum

$$\Psi_a(\omega) = \sqrt{\Lambda_a'(\omega)}\Psi[\Lambda_a(\omega)]. \tag{14}$$

$\psi_a(n)$ is also bandlimited and the two ends of the pass band are given by

$$\omega_1' = 2\tan^{-1}[\tan(\omega_1/2)/a] \text{ and } \omega_2' = 2\tan^{-1}[\tan(\omega_2/2)/a]. \tag{15}$$

If $0 < a < 1$, then $\omega_1' \ge \omega_1$ and $\omega_2' \ge \omega_2$, the whole pass band shifts to the right. If $a > 1$, then the whole pass band shifts to the left. Along with the shifting of the whole pass band in one direction, the bandwidth of the pass band also changes. Let $\Delta\omega$ and $\Delta\omega'$ be the bandwidths of the mother wavelet $\phi(n)$ and the wavelet $\phi_a(n)$. It is found that

- If $0 < a < 1$, then

$$\begin{cases} \Delta\omega' > \Delta\omega & \text{if } \tan(\omega_1/2)\tan(\omega_2/2) < a \\ \Delta\omega' = \Delta\omega & \text{if } \tan(\omega_1/2)\tan(\omega_2/2) = a \\ \Delta\omega' < \Delta\omega & \text{otherwise} \end{cases}$$

- If $a > 1$ then

$$\begin{cases} \Delta\omega' > \Delta\omega & \text{if } \tan(\omega_1/2)\tan(\omega_2/2) > a \\ \Delta\omega' = \Delta\omega & \text{if } \tan(\omega_1/2)\tan(\omega_2/2) = a \\ \Delta\omega' < \Delta\omega & \text{otherwise} \end{cases}$$

In the first example of the next section, $\omega_1 = 0$ and $\omega_2 = \pi/2$. As a changes, ω_1 remains at the origin, while ω_2 shifts to the right if $0 < a < 1$ and shifts to the left if $a > 1$. This gives a dilated frequency spectrum and thus a compressed wavelet when $0 < a < 1$, and a dilated wavelet when $a > 1$. In the second example, $\omega_1 = \pi/4$ and $\omega_2 = 3\pi/4$. Note that $\tan(\omega_1/2)\tan(\omega_2/2) = 1$. It is found that $\Delta\omega' < \Delta\omega$ for both $0 < a < 1$ and $a > 1$. Therefore, if $0 < a < 1$, both ω_1 and ω_2 shift to the right and the bandwidth decreases; if $a > 1$, both ω_1 and ω_2 shift to the left and the bandwidth still decreases. This eventually results in a compressed wavelet when $0 < a < 1$ and a dilated wavelet when $a > 1$.

Example 1: $\omega_1 = 0, \omega_2 = \pi/2$

Consider a discrete-time DCWT mother wavelet $\psi(n)$ which has the following frequency spectrum in $[-\pi, \pi]$

$$\Psi(\omega) = \begin{cases} |\sin(2\omega)| & \text{if } |\omega| \in [0, \pi/2] \\ 0 & \text{otherwise} \end{cases} \tag{16}$$

The spectrum $\Psi_a(\omega)$ of the DCWT wavelet at scale a is

$$\Psi_a(\omega) = \begin{cases} \left| \frac{2a\sqrt{a}\sin(\omega)[\cos^2(\omega/2) - a^2\sin^2(\omega/2)]}{[\cos^2(\omega/2) + a^2\sin^2(\omega/2)]^{5/2}} \right| \\ \qquad \text{if } |\omega| \in [0, 2\tan^{-1}(\frac{1}{\sqrt{2}a})] \\ 0 \qquad \text{otherwise} \end{cases} \tag{17}$$

The spectrum $\hat{\Psi}_a(\omega)$ of the IDCWT wavelet at scale a is

$$\hat{\Psi}_a(\omega) = \begin{cases} \left| \frac{8a\sqrt{a}\sin^2(\omega/2)\sin(\omega)[\cos^2(\omega/2) - a^2\sin^2(\omega/2)]}{[\cos^2(\omega/2) + a^2\sin^2(\omega/2)]^{5/2}} \right| \\ \qquad \text{if } |\omega| \in [0, 2\tan^{-1}(\frac{1}{\sqrt{2}a})] \\ 0 \qquad \text{otherwise} \end{cases} \tag{18}$$

Figure 2 shows the example DCWT mother wavelet and DCWT wavelets at different scales. Figure (3) shows the example IDCWT mother wavelet and IDCWT wavelets at different scales. The IDCWT constant in this case is $C_\psi = 4/3$. Figure 4 shows the scalogram of the DCWT of a chirp function [3]

$$x(n) = \sin[\pi n^2/(2N)], \text{ for } n = 0, 1, ..., N \tag{19}$$

using this wavelet. The continuous changing of the frequency is apparent.

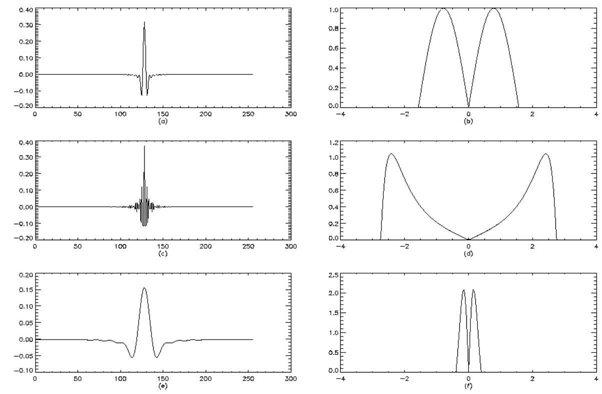

Figure 2: Example of DCWT bandlimited wavelet for the bilinear case. The pass band is located between $\omega = 0$ and $\omega = \pi/2$. (a) the DCWT mother wavelet; (c) DCWT wavelet at scale $a = 0.2$; (e) DCWT wavelet at $a = 5$; (b) (d) (f) frequency spectra of (a) (c) (e) respectively.

Example 2: $\omega_1 = \pi/4, \omega_2 = 3\pi/4$

The frequency spectrum of the DCWT mother wavelet in this example is given by

$$\Psi(\omega) = \begin{cases} |\cos(2\omega)| & \text{if } |\omega| \in [\pi/4, 3\pi/4] \\ 0 & \text{otherwise} \end{cases} \tag{20}$$

The DCWT wavelet at scale a has the following spectrum.

$$\Psi_a(\omega) = \begin{cases} \left| \frac{\sqrt{a}[\cos^4(\omega/2) + a^4\sin^4(\omega/2) - 3/2\sin^2(\omega)]}{[\cos^2(\omega/2) + a^2\sin^2(\omega/2)]^{5/2}} \right| \\ \qquad \text{if } |\omega| \in [2\tan^{-1}(\frac{\pi}{8}), 2\tan^{-1}(\frac{3\pi}{8})] \\ 0 \qquad \text{otherwise} \end{cases} \tag{21}$$

The frequency spectrum of the IDCWT wavelet at scale a is given by

$$\Psi_a(\omega) = \begin{cases} \left| \frac{4\sqrt{a}\sin^2(\omega)[\cos^4(\omega/2) + a^4\sin^4(\omega/2) - 3/2\sin^2(\omega)]}{[\cos^2(\omega/2) + a^2\sin^2(\omega/2)]^{5/2}} \right| \\ \qquad \text{if } |\omega| \in [2\tan^{-1}(\frac{\pi}{8}), 2\tan^{-1}(\frac{3\pi}{8})] \\ 0 \qquad \text{otherwise} \end{cases} \tag{22}$$

The IDCWT constant is $C_\psi = 0.558$. Figure 5 and 6 show plots of these DCWT and IDCWT wavelets at different scales. By changing the value of a and correlating the wavelet thus obtained with a given signal, different regions of the frequency spectrum of the given function are covered by the DCWT.

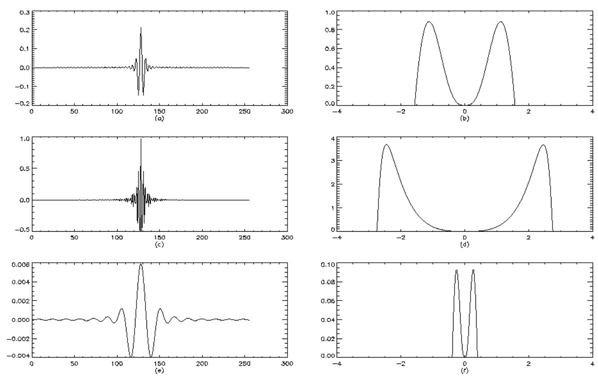

Figure 3: Example of IDCWT bandlimited wavelet for the bilinear case. The pass band is located between $\omega = 0$ and $\omega = \pi/2$. (a) the IDCWT mother wavelet; (c) IDCWT wavelet at scale $a = 0.2$; (e) IDCWT wavelet at $a = 5$; (b) (d) (f) frequency spectra of (a) (c) (e) respectively.

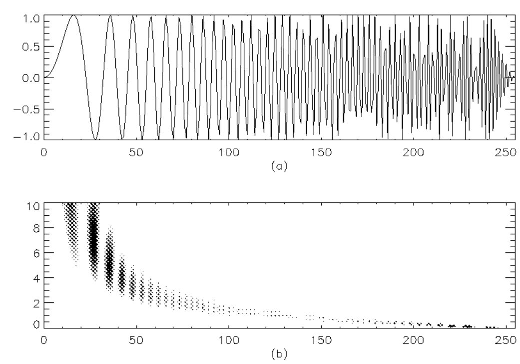

Figure 4: DCWT of a chirp function. (a) input; (b) scalogram of the DCWT.

4. CONCLUSION

The DCWT and IDCWT framework presented in this paper offers advantages in that it uses a set of discrete-time wavelets and is able to accommodate continuous dilations of the mother wavelet to provide analysis and synthesis of a discrete-time signal. It provides a potential tool for applications such as pattern recognition, image processing, etc., that require information of dilations of a discrete signal at arbitrary scaling factors.

5. REFERENCES

[1] I. Daubechies. Orthonormal bases of compactly supported wavelet. *Commun. Pure Appl. Math.*, 41:909–996, Nov. 1988.

[2] I. Daubechies. *Ten Lectures on Wavelets*. SIAM, 1992.

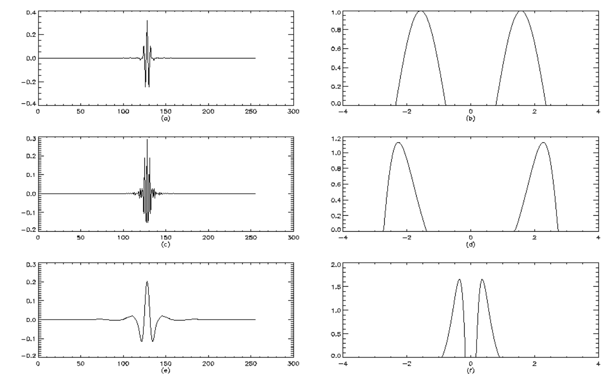

Figure 5: Example of DCWT bandlimited wavelet for the bilinear case. The pass band is located between $\omega = \pi/4$ and $\omega = 3\pi/4$. (a) the DCWT mother wavelet; (c) DCWT wavelet at scale $a = 0.5$; (e) DCWT wavelet at $a = 5$; (b) (d) (f) frequency spectra of (a) (c) (e), respectively;

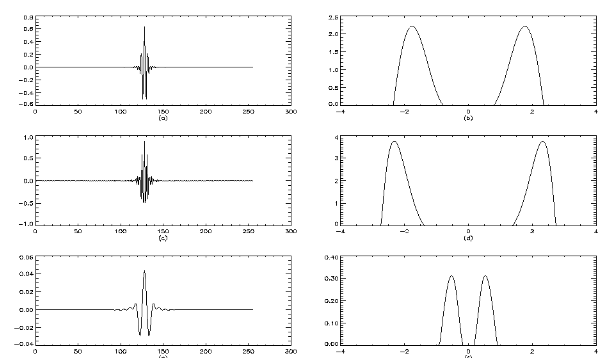

Figure 6: Example of IDCWT bandlimited wavelet for the bilinear case. The pass band is located between $\omega = \pi/4$ and $\omega = 3\pi/4$. (a) the IDCWT mother wavelet; (c) IDCWT wavelet at scale $a = 0.5$; (e) IDCWT wavelet at $a = 5$; (b) (d) (f) frequency spectra of (a) (c) (e) respectively;

[3] D. J. Gaskill. *Linear Systems, Fourier Transforms, and Optics*. John Wiley & Sons, 1978.

[4] A. D. Poularikas and S. Seely. *Signals and Systems*. PWS-KENT, Boton, 1991.

[5] M. J. Shensa. The discrete wavelet transform: Wedding the a trous and mallat algorithms. *IEEE Trans. on Signal Processing*, 40(10):2464–2482, Oct. 1992.

[6] G. Strang. Wavelets and dilation equations: A brief introduction. *SIAM Review*, 31:614–627, Dec. 1989.